Nuclear Instruments and Methods in Physics Research B 319 (2014) 100–106

Contents lists available at ScienceDirect

Nuclear Instruments and Methods in Physics Research B

journal homepage: www.elsevier.com/locate/nimb

2.6 MeV proton irradiation effects on the surface integrity of depleted UO_2

J. Pakarinen [a,*], L. He [a], M. Gupta [a], J. Gan [b], A. Nelson [c], A. El-Azab [d], T.R. Allen [a,b]

[a] University of Wisconsin – Madison, Department of Engineering Physics, Madison, WI 53706, USA
[b] Idaho National Laboratory, Idaho Falls, ID 83415, USA
[c] Los Alamos National Laboratory, Los Alamos, NM 87545, USA
[d] Purdue University, School of Nuclear Engineering, West Lafayette, IN 47907, USA

ARTICLE INFO

Article history:
Received 13 September 2013
Received in revised form 18 November 2013
Available online 5 December 2013

Keywords:
Uranium dioxide
Proton irradiation
Surface flaking
Crystal damage

ABSTRACT

The effect of low temperature proton irradiation in depleted uranium dioxide was examined as a function of fluence. With 2.6 MeV protons, the fluence limit for preserving a good surface quality was found to be relatively low, about 1.4 and 7.0 × 10^{17} protons/cm^2 for single and poly crystalline samples, respectively. Upon increasing the fluence above this threshold, severe surface flaking and disintegration of samples was observed. Based on scanning electron microscopy (SEM) and X-ray diffraction (XRD) observations the causes of surface failure were associated to high H atomic percent at the peak damage region due to low solubility of H in UO_2. The resulting lattice stress is believed to exceed the fracture stress of the crystal at the observed fluencies. The oxygen point defects from the displacement damage may hinder the H diffusion and further increase the lattice stress, especially at the peak damage region.

Published by Elsevier B.V.

1. Introduction

The properties of UO_2, the most common ceramic nuclear fuel, degrade during fuel use in nuclear reactors due to complex microstructure evolution processes. At high burnup levels or elevated temperature, the thermal conductivity of UO_2 decreases from an already low initial value, which impacts the microstructure evolution in fuel assisted by high radial temperature gradients [1]. Fuel irradiation also leads to the accumulation of gaseous and solid fission products, defect clusters and dislocations in the UO_2 matrix [2]. In addition to these microstructural features, the high radioactivity of spent fuel makes the post-irradiation characterization of actual fuel material challenging. To mimic the processes taking place in real nuclear fuel while controlling the microstructure and without having to deal with high radioactivity, ion irradiations have been applied to examine the changes in the microstructures of depleted UO_2. Depending on the applied ion type, energy, and fluence, the resulting microstructures consist of varying amounts gas bubbles, voids, precipitates, and dislocation loops and networks [3,4]. However, the resulting microstructure can be regulated to some extent either during irradiation or annealing to understand the interplay between the damage process, defect processes and microstructure changes.

Irradiation of UO_2 is often performed with fission-relevant ions such as krypton (Kr) or xenon (Xe) ions, while light H and He ions are common for irradiating fusion related ceramics, such as SiC and Al_2O_3 [4,5]. However, He ions are also relevant for UO_2 irradiation as alpha particles are generated as fission or decay products in nuclear fuel, and tritium, ^3H, a hydrogen isotope, also exist in UO_2 as a fission product [6]. The behavior of He^+ and He^{2+} in UO_2 has been previously studied [6,7]. Most distinctly, the low-dose damage region (<0.1 dpa) in He irradiated UO_2 shows an increase in the lattice parameter, which has been attributed to the formation of isolated Frenkel pairs [7]. Recent results from spatially resolved Raman examinations indicate that the high dose (>1 dpa) microstructure of He implanted UO_2 includes a different type of defect; namely, U_4O_9 type defect clusters were proposed [8]. The formation of U_4O_9 is generally related to oxidation of UO_2 [9] and, therefore, must be related to oxygen point defect accumulation near the peak damage region. Clearly, the point defect kinetics plays a critical role in the damage left in UO_2 by irradiation.

The current investigation focuses on proton (H^+) irradiation of single crystal and polycrystalline UO_2. Similar studies on proton irradiation of depleted UO_2 have not been reported before. The objectives of this investigation are to create a bulk-like defect microstructure in UO_2, and to study the fluence limits for performing such irradiation at low temperature without damaging the samples. Protons with energy of 2.6 MeV were used to achieve a damage plateau of approximately 32 µm. The irradiation temperature was kept as low as possible to freeze the damage produced

---

* Corresponding author. Tel.: +1 608 262 7476.
E-mail address: pakarinen@wisc.edu (J. Pakarinen).

0168-583X/$ - see front matter Published by Elsevier B.V.
http://dx.doi.org/10.1016/j.nimb.2013.11.014

and to enable a comparison with low temperature He irradiation. Our observations showed that the UO_2 crystal integrity deteriorated with a relatively small H^+ fluence. The findings are discussed here based on X-ray diffraction and scanning electron microscopy studies of the irradiated samples.

2. Materials and methods

Single crystalline and polycrystalline depleted UO_2 samples were examined. The single crystalline UO_2 samples were fabricated at the Chalk River Laboratories by heating fused UO_2 with hyperstoichiometric UO_2 at 1900 K under a hydrogen atmosphere. The lattice constant $a = 5.473 \pm 0.001$ Å was determined by neutron scattering measurements at room temperature, which indicates that the O/U was very close to 2 [10]. The polycrystalline samples were sintered at Los Alamos National Laboratory. Feedstock powders were prepared by milling depleted UO_2 powder with 0.25 wt.% ethylene bis-stearamide in an alumina SPEX mill for 15 min before sieving through a 200 screen mesh. Typical powder impurities were below the detection limit of the inductively coupled mass spectrometer measurement, with the exception of 11 ppm Al content. Approximately 1 g of powder was pressed in a 6.22 mm single action die at roughly 80 MPa, held for 60 s. Densification was then performed in a tungsten metal furnace. Green pellets were placed on tantalum foil inserted on top of tungsten furnace trays. Pellets were sintered under an argon atmosphere containing 5–10 ppm oxygen for 4 h at 1650 °C. The atmosphere was then switched to argon containing 6% hydrogen during cooling in order to obtain stoichiometric UO_2. The above process produced dense pellets measuring roughly 5.2 mm in diameter and 4.3 mm in height, and found to be between 95% and 96% of the theoretical density. The pellets were sliced to 0.6 mm thick disks with a low speed diamond saw and polished to mirror finish using diamond suspensions (15–0.25 μm) prior ion irradiations. After cutting into 0.6 mm slices, 3 mm disks were core drilled from the single crystals and polished to mirror finish prior ion irradiation.

A toroidal volume ion source (TORVIS) produced H^+ ions for the irradiation. The ions were accelerated to 2.6 MeV by a Pelletron® tandem accelerator at the University of Wisconsin – Madison. The sample temperature was monitored through the irradiations with two thermocouples connected across the stage. The beam was rasterized across the sample region to achieve a uniform distribution of ions over the specimen. Beam current and specimen temperature were recorded throughout the irradiations. The temperature, as indicated by the thermocouples, was under 400 °C for single crystals and under 300 °C for polycrystalline samples. No outer heating source was applied during the irradiations (beam heating only). Table 1 summarizes the irradiation details for the samples. The single crystalline samples were mounted on a molybdenum sample holder, capable of holding altogether 12 disks simultaneously. Two disks were first irradiated to a fluence of 1.41×10^{17} H^+/cm^2 and altogether eight disks were irradiated to 7.05×10^{17} H^+/cm^2. The plan of the experiment was to continue the single crystalline series to higher fluencies, by removing two samples at a time and continuing the irradiation with the rest, but the crystal deterioration at 7.05×10^{17} H^+/cm^2 prevented further irradiations. The poly crystalline samples were fixed onto a Cu holder, two samples at a time, and irradiated to 1.41×10^{17}, 7.05×10^{17}, and 1.41×10^{18} H^+/cm^2. Also, the series was limited by surface flaking at the highest fluence. The Stopping and Range of Ions in Matter (SRIM) computer code was used to simulate the profiles of atomic displacements in UO_2 as a function of depth [11]. The threshold displacement energies for oxygen and uranium were set to 20 and 40 eV, respectively, and the simulation was performed in the "quick" Kichin-Peace damage calculation mode [12]. The depth-dependent displacement damage and H atomic percent as a function of fluence are shown in Fig. 1(a) and (b), respectively. The peak and plateau values are collected to Table 1 to facilitate the comparison between samples in Section 3.

The samples were examined before and after irradiations by X-ray diffraction (XRD) and scanning electron microscopy (SEM). A JEOL 6610 SEM at 20 kV and Siemens Stoe X-ray diffractometer using Cu K_α radiation (40 kV, 2.5 mA) was used in omega-2theta geometry.

3. Results and discussion

3.1. SEM and XRD observations

SEM observations for the proton irradiated single crystalline samples are shown in Fig. 2. The 1.41×10^{17} H^+/cm^2 sample does not show any signs of surface deterioration, Fig. 2(a), while severe surface flaking is evident for the 7.05×10^{17} H^+/cm^2 sample, Fig. 2(b). Altogether eight samples were irradiated to 7.05×10^{17} H^+/cm^2 and they all showed similar laminar type cracking. A magnified view of the cracked surface is shown in Fig. 2(c). Although the fracture clearly took place in sequences and the cracking surface is parallel to the original surface, no clear evidence of crack propagation along a particular crystal orientation was detected.

A SEM comparison of the polycrystalline samples, which survived either annealing of 30 h at 300 °C under vacuum or the low-dose irradiation, is shown in Fig. 3. No deleterious effects were observed with annealing, Fig. 3(a) and (b), but the grain boundaries showed slightly increased contrast, which most likely is related to thermal relaxation. The lowest fluence irradiations ($1.41 \times 10^{17}$and 7.05×10^{17} H^+/cm^2), Fig. 3(c)–(f), did not show any major differences either, although the irradiated region was clearly seen as a slight contrast variation on the disk edges. Unlike the single crystal samples, the polycrystalline UO_2 samples irradiated to 7.05×10^{17} H^+/cm^2 did not suffer any surface damage.

Upon increasing the fluence to 14.1×10^{17} H^+/cm^2 an obvious threshold for surface flaking was reached. Fig. 4 shows the polycrystalline samples upon irradiation. While one of them, Fig. 4(a), lost the major part of its surface, the second had a large amount of radial cracks, Fig. 4(b) and (d), propagating from the edge of the disk to the center. Also, as can be observed by the naked-eye, the sample surface seemed to be slightly elevated from the

Table 1
Sample and irradiation matrix. A minimum of two samples for each fluence were irradiated. The dpa and H at.% values are from SRIM simulations. The plateau values were taken from the depth of 15 μm.

Sample ID	PC/SC	Fluence ($\times 10^{17}$ H/cm^2)	dpa (plateau)	H at.% (plateau)	dpa (peak)	H at.% (peak)	Time (h)	T (°C)
SC-1,2	SC	1.41	0.01	0.0005	0.14	0.84	2	<400
SC-3–10	SC	7.05	0.05	0.0025	0.68	4.20	10	<400
PC-1,2	PC	1.41	0.01	0.0005	0.14	0.84	2	<300
PC-3,4	PC	7.05	0.05	0.0025	0.68	4.20	10	<300
PC-4,5	PC	14.1	0.1	0.0050	1.38	8.40	20	<300
PC-6,7	PC	0	0	0	0	0	20	300

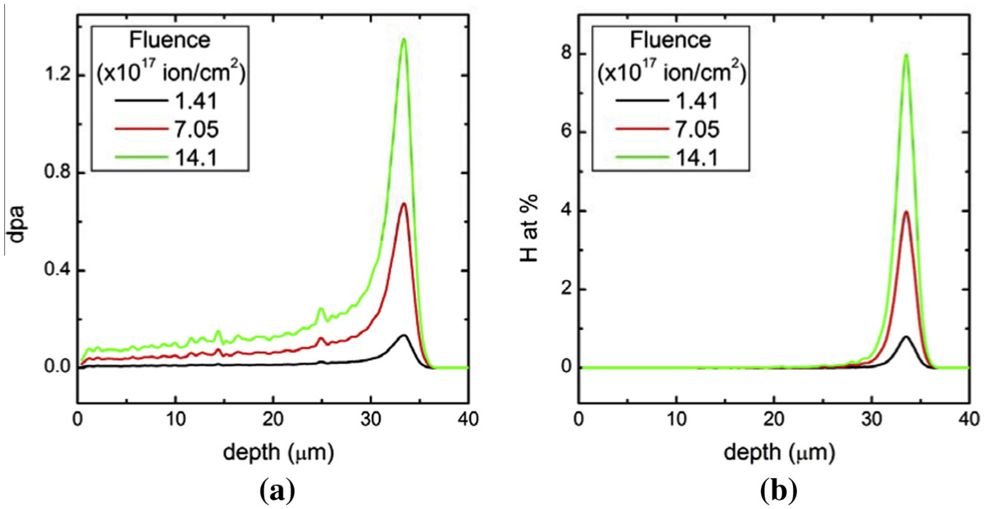

(a) (b)

Fig. 1. SRIM simulation results for (a) displacement damage and (b) the atomic percent of implanted H (b) as function of ion fluence.

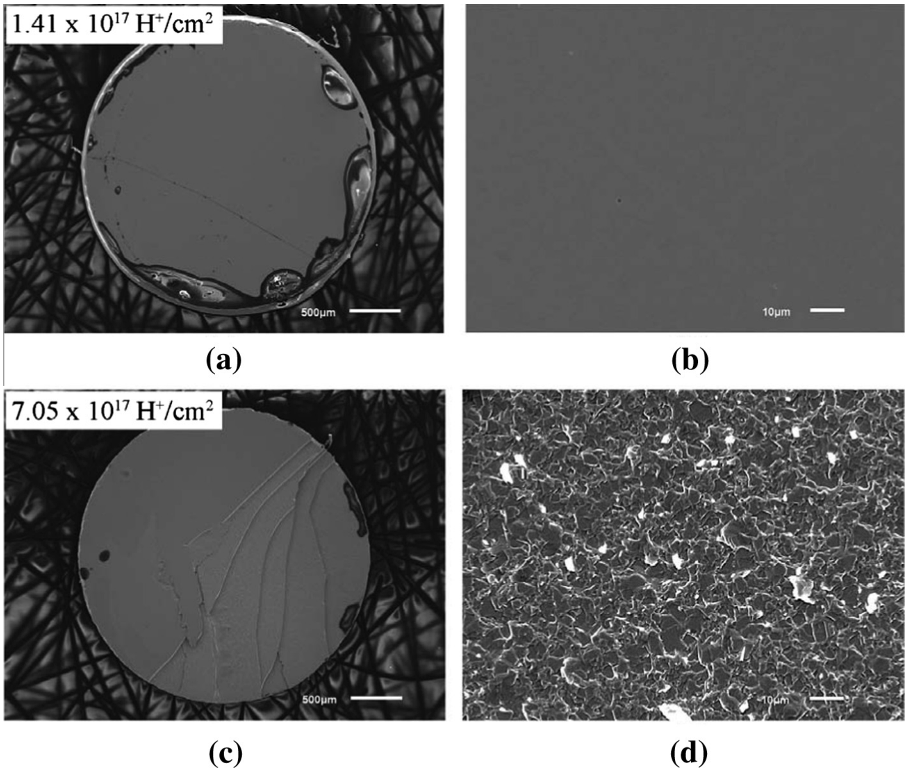

(a) (b) (c) (d)

Fig. 2. Single crystal UO_2 samples showed no signs of surface deterioration in (a) low or (b) high SEM magnification after being irradiated to a fluence of 1.41 × 10^{17} H^+/cm^2 (0.01 dpa plateau). (c) To the contrary, laminar disintegration took place upon increasing the fluence to 7.05 × 10^{17} H^+/cm^2. (d) The fracture surface was rough and did not indicate fracture in any specific crystal direction.

irradiated region, further confirming the surface layer being very close of blistering. A high magnification image from the bottom of the blister revealed it being cracked partly intergranularly, Fig. 4(c) and (e). The irradiated but non-blistered surface, Fig. 4(f), did not show any major differences as compared to the low-dose or annealed intact samples. The observations imply that the sample deterioration was most likely related to the irradiation effects at the peak damage region.

XRD scans were recorded for the polycrystalline samples before and after irradiations. The results for the (224) peak are shown in Fig. 5. The (224) peak was chosen for the comparison due to its larger probing depth as compared to reflections at lower 2θ angles [13]. The vacuum annealing, as expected, did not shift the peak in any direction, which implies no change in the sample stoichiometry. The proton irradiation, however, produced a clear shift of the diffraction peaks to smaller 2θ angles as compared to the un-irradiated reference sample. The largest peak shift was observed when the XRD was measured from the center of the blistered sample (fluence 14.1 × 10^{18} ion/cm^2). A thorough analysis of the XRD results, including extensive modeling work, will be published elsewhere, but a few conclusions from the results can be drawn. First, the observed lattice expansion is in agreement with studies done for He^{2+} irradiated UO_2, [7] but the magnitude with H^+ is much smaller, Fig. 6. Therefore, it's unlikely that the defects at the

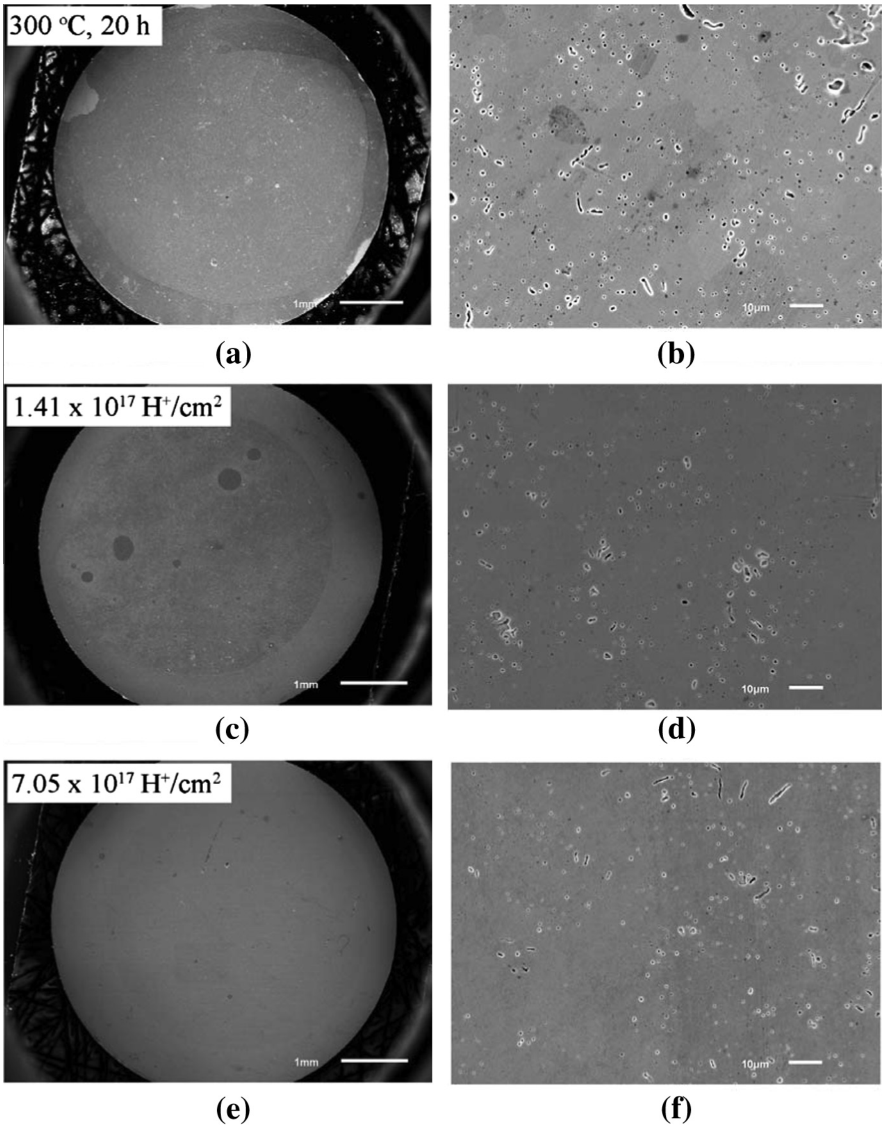

Fig. 3. Polycrystalline UO_2 samples did not show any indication of surface rupture upon (a) annealing 30 h at 300 °C, (c) irradiation to 1.41×10^{17} H^+/cm^2 (0.01 dpa plateau), or (e) irradiation to 7.05×10^{17} H^+/cm^2 (0.05 dpa). Corresponding high magnification SEM images (b), (d), and (f) confirmed that the surfaces were intact in all cases.

plateau region are responsible for the crystal deterioration. Secondly, the fact that the biggest shift in XRD was seen in the cracked sample indicates that the cracking must take place at or close to the peak damage region (continuing the linear lattice expansion trend, it would require a fluence corresponding to dose of ~0.2 dpa at the plateau, which is not reasonable with the current experiment, Fig. 1(a)).

3.2. The role of displacement damage and H concentration

According to SRIM simulations, Fig. 1(a), the maximum displacement damage with 2.6 MeV H+ ions occurs at about 32 μm beneath the sample surface. The plateau region before the peak damage is fairly homogeneous and increases as function of fluence. The maximum peak damage at the highest applied fluence (1.41×10^{18} H/cm^2) was about 1 dpa. UO_2 is one of the most irradiation tolerant materials known. Commercial nuclear fuel pellets, for example, are subjected to roughly 1 dpa per day under nuclear power plant operation, while the fuel cycle is in the range of several years [14]. Spent nuclear fuel thus experiences a dose of thousands of dpa's. The high dose of spent nuclear fuel does affect the pellet microstructures and integrity, but the main effects are not prominent before ~4 years of operation (~1500 dpa). [14] Similarly, heavy-ion irradiations have shown that despite microstructural evolution in UO_2 at relatively small doses, the sample integrity is not lost even with tens of dpa's [4]. The peak displacement damage in this work with H ions was about 1 dpa. Taking into consideration all the above said, the displacement damage seems unlikely to explain the deterioration for the UO_2 crystals upon the peak damage of 0.5 and 1 dpa for single and polycrystalline samples, respectively. However, the low irradiation temperature may drastically change the defect annihilation and crystal recovery. Further discussion on defect accumulation is given in Section 3.3.

Similar to the displacement damage, the H atomic percent peaks at the depth of 32 μm, Fig. 1(b), being about 8 atomic percent upon the highest fluence. The SRIM calculation does not take into account H diffusion within the UO_2 crystal during irradiation, but gives the concentration as if all the implanted H ions would remain in the crystal at the points where they come to a complete stop. The role of H in blistering of ceramic materials has been extensively studied but the main emphasis being fusion related

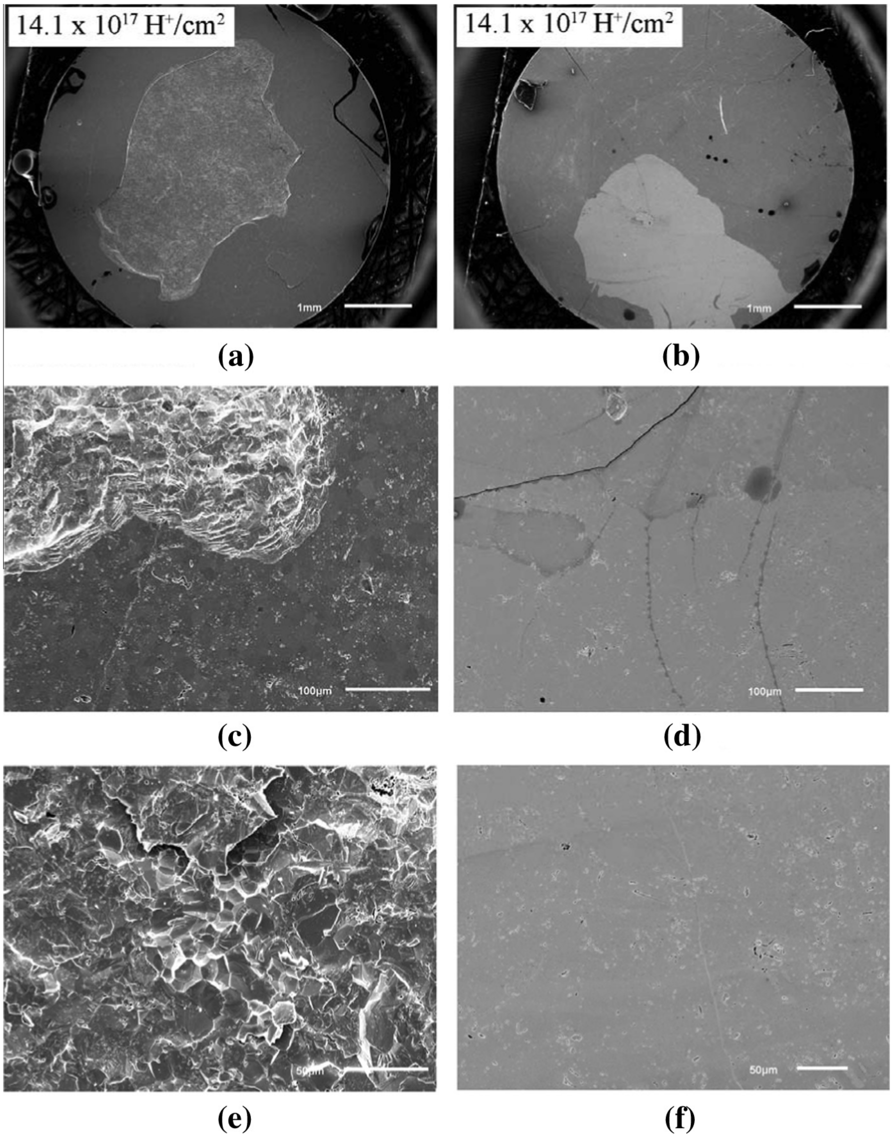

Fig. 4. Polycrystalline UO_2 suffered severe surface flaking when the fluence was increased to 14.1 × 10^{17} H^+/cm^2 (0.1 dpa plateau). One sample lost most of its surface, (a) while the second showed large amount of radial cracks, (b) and elevated surface layer. The bottom of the blister, (c) showed similar rough feature as the SC samples, but also locations where intergranular cracking had taken place (e). Acetone residuals showed the locations of the small cracks (d). Notably, the sample surfaces at the intact locations resembled the annealed and low-dose samples (f).

materials and electronics [5]. For UO_2, hydrogen solubility and diffusion studies have mainly been motivated by pellet fabrication, related H infusion and subsequent release effects on the Zr cladding [15]. A common conclusion can be drawn from these earlier studies; the solubility of H is very low in ceramics. In particular, the solubility of H in UO_2 has been found to be extremely low, the crystal can take only about 0.4 μg H_2/g UO_2 [15]. On the other hand, H diffusion in UO_2 has been found to be extremely fast; the temperature dependent diffusion coefficient for H (D_H) is on the range of 3.5×10^{-6} cm^2/s at 500 °C [15]. As a comparison, O diffusion coefficient in UO_2 at the same temperature (D_O) is in the range of 10^{-8} cm^2/s [16]. The ratio between the diffusion coefficients, $D_H/D_O \sim 350$ (at 500 °C) indicates that H diffusion is rapid in UO_2. However, the diffusion and solubility experiments have been done by infusion methods without the presence of irradiation damage. For example, microstructural observations from H irradiated ceramics have shown that H has a tendency to pile up and form sharp plane-like cavities at the peak damage region [5]. Furthermore, the depth of the peak damage region (and also peak H) was fairly large in this work, 32 μm, which may play a critical role in H out diffusion. Also, due to the low solubility of H in UO_2, the precipitation of H_2 molecules from the implanted H^+ ions may further decrease the H diffusion. Summarizing the above said; even though H diffusion in UO_2 should be extremely rapid the H build up at the peak damage region is the most likely reason for the observed sample surface failures.

3.3. UO_2 phase stability and postulated scenarios of sample damage

While the H pile-up at the peak deposition range appears to be the most probable cause for the observed surface fracture, recent spatially resolved investigations have shown that the defect types of UO_2 vary as a function of displacement damage [8]. Interestingly, the regions with higher damage (and implanted gas) show signs of defects, which have been proposed to originate from the formation of U_4O_9 type of clusters [8]. While oxidation of UO_2 during H (or He) irradiation is unlikely due to high vacuum environment, UO_2 is known to have multiple O-rich phases in the

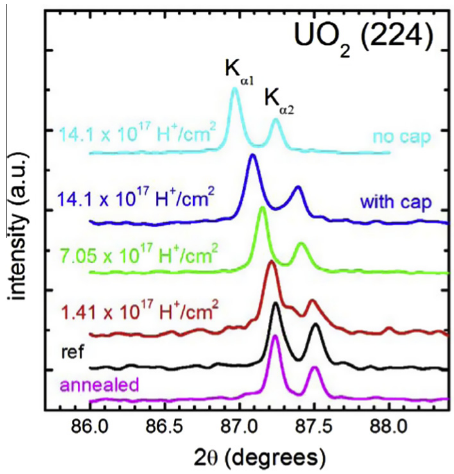

Fig. 5. X-ray diffraction for the polycrystalline samples showed a clear fluence-dependent shift of the (224) diffraction peak to the smaller 2θ angle as compared to the reference or annealed sample. The sample with the surface blistered off showed the highest peak shift.

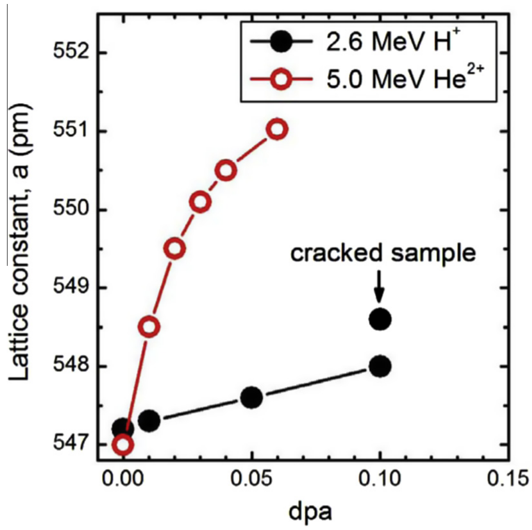

Fig. 6. Lattice constants calculated based on the position of the (224) peak showed relatively linear trend for the lattice expansion of H^+ irradiated samples. The behavior is similar to the He^{2+}, but the effect of H is much smaller than He^{2+}. The He^{2+} data is extracted from [7].

oxygen rich conditions [9]. In general, when U_4O_9 phase (sometimes a mixture of U_4O_9/U_3O_7) is formed on the surface of UO_2, it does not lead to crystal fracture, but is known to initiate the formation of U_3O_8 [17]. Unlike the U_4O_9 phase, U_3O_8 has a completely different crystal structure than UO_2 (the net volume increase upon phase transformation is ~36%. As such, when formed on top of UO_2/U_4O_9, U_3O_8 flakes off [17]. The flaking of U_3O_8 is especially a problem with the activated spent nuclear fuel. If the irradiation damage causes oxygen rich and oxygen depleted local structures in the UO_2 matrix, the stability of those features under irradiation may play a role in the fracture behavior.

The X-ray diffraction observations in this work, although done in relatively high angle, were limited to about 1.2 μm probing depth [13] and the observed features therefore do not give information about the phases or stresses present at the peak damage regions of the crystals. The XRD from the sample with blistered off surface (Fig. 5) did not show any additional peaks which could have been related to U_4O_9 or U_3O8, but as stated earlier, they may have been flaked off from the UO_2 when the sample has failed. While the experimental evidences of a UO_2 phase transformation at the peak damage level could not been found (due to reasons explained above), the possibility and consequences are discussed here on theoretical grounds.

We postulate a number of possible causes for the fracture of UO_2 surfaces under proton irradiation past a certain threshold, as shown in Figs. 2 and 4. In discussing these causes, the difference between single and polycrystalline UO_2 is kept in mind. With regard to the single crystal response, fracture of the type shown in Figs. 2 and 4 is associated with a mechanical stress that exceeds the fracture strength of the material. In the absence of a direct mechanical loading, stresses arise in samples due to the free volume changes associated with the creation of defects and phase changes. Stresses may also arise due to accumulation of charge and the Coulomb repulsion associated with such changes. In electrically grounded samples, it is assumed that the charge associated with the ion current is somewhat neutralized instantly. It is also assumed here that the temperature of the sample is uniform and no significant temperature gradients are presents. We are thus left with stresses associated with the free volume of defects and phase changes. As Fig. 1 indicates the deposition profile of the H^+ ions shows a highly localized peak at about 32 μm. The concentration at this peak varies more or less linearly with the dose, and it rises to about 8 at.% at 14×10^{17} ions/cm^2. This is considered a high concentration, well above the solubility limit of H in UO_2. Setting aside the lattice damage associated with H insertion, which also peaks at the same range as H ion deposition, the free volume change associated with H insertion in UO_2 can be significant. Assuming that the material expands uniformly over a layer of one to two microns thickness at a depth of ~32 μm, stress build up due to this expansion is expected, and the laminar fracture pattern observed can be explained accordingly. The level of stress can vary depending on how much H diffusion has occurred, both in the inward and outward directions from the peak deposition layer. The fact that the peak damage profile occurs more or less at the same range as the H deposition makes possible the entrapment of H ions and lessens the extent of diffusion of inserted ions. The compound effect of defect creation and entrapment of H ions in a narrow region is likely the direct cause of the observed fracture.

The above scenario discards the effect of damage and assumes stress build up to be fully due to free volume expansion associated with H insertion. Another possible scenario may also be suggested. Because of the significant mass asymmetry, it is anticipated that more O atoms are displaced in UO_2 than U atoms. As such, the peak damage region will be viewed as a source of O interstitials, which can migrate out of that region, both inward and outward, and lead to the enrichment of the solid layers on both side of the damage layer with O, effectively leading to oxidation of the material on both sides of the peak damage region. The excess oxygen will result in a change in the lattice parameter [18] and the creation of a lattice mismatch. The resulting stress can, again, lead to the observed fracture pattern in the case of single crystal. Which of the above two scenarios is more effective in creating the observed damage is a matter of further studies of the fate of H ions inserted in the material, and how the created damage contribute to the distribution of these ions and the displaced O atoms. This scenario depends on whether the irradiation temperature, which is kept below 400 °C enables enough oxygen diffusion in the samples in the vicinity of the peak damage region.

It remains to explain the difference between the observed stability of the polycrystalline UO_2 samples relative to the single crystal counterpart. It seems that the presence of grain boundaries makes the material less susceptible to the irradiation induced fracture. This may be explained as follows. In the case of single crystal UO_2, it seems that the creation of stress at the peak deposition depth leads to flaking off of a uniform layer of thickness more or less equal to the peak damage of deposition depth. It is anticipated that the fracture surface can be smooth at the large scale with some granular features at small scale. In the case of poly crystalline samples, the depth of deposition may vary slightly from one grain to another depending on the grain orientations. This makes it possible for peak damage layer to be a bit more diffuse and the resulting stresses to be a bit less concentrated. The level of stress itself may also be lower in the case as grain boundary can provide fast diffusion path for the inserted ions, which distributes them more in the material. The presence of pores in the polycrystalline samples can also serve as a mechanism of resistance to fracture because these pores can accommodate a fraction of the inserted H.

From the experimental point of view, the observations clearly indicate that the study of point defect evolution in UO_2 cannot be done to high dpa's with single proton beam energy due to the deterioration taking place at the peak damage region. Efforts are now directed to rotating the sample surface against the ion beam incidence and to varying the incoming ion beam energy. Based on the H at.% limits observed at peak damage regions in this work, the fluencies and energies may be determined in such a way that the crystal is not stressed beyond its limits. Yet, creating a deep and homogenous defect plateau in UO_2 by ion irradiation remains as a complicated task. The samples irradiated to a low displacement dose in this work will suffice for experiments, which have a high resolution for the defect morphology and the ability to select the depth of the examined region (such as transmission electron microscopy or X-ray absorption spectroscopy). Furthermore, to clarify the H behavior and irradiation damage evolution in UO_2 (H bubble formation, lattice recovery, characterization of irradiation damage) post-irradiation annealing accompanied by TEM and XRD examinations will be considered as further work for these samples.

4. Conclusions

Single and polycrystalline depleted UO_2 disks were irradiated with 2.6 MeV protons until surface blistering took place. The maximum fluencies were found to be relatively low, only about 7.0 and 14.1×10^{17} protons/cm^2 for poly and single crystalline samples, respectively. The SEM observations indicate that the deterioration took place at the peak damage region of the crystals. The most probable reason for the sample deteriorations was concluded to be H pile-up at the peak damage regions and subsequent laminar stress. The fact that the polycrystalline samples could be irradiated to a higher fluence than the single crystalline samples indicates that the grain boundaries may help in distribution the inserted H atoms via grain boundary diffusion. The intergranular fracture surface observed at the blisters of the polycrystalline sample indicates that the grain boundaries may have an effect on stress development inside the crystal. Also, the 5% porosity is likely to help to accommodate more H into the polycrystalline samples.

While no experimental evidence for phase transformation was detected, the possibility was considered theoretically. Recent results from Raman experiments [8] have shown that irradiation related to changes in the oxygen sub lattice may be present at the peak damage region of He implanted UO_2 samples. Similar behavior in the H+ irradiated samples could induce a flux of oxygen defects to the surroundings of the peak damage region and induce changes in the phase of UO_2 locally and possibly further hinder the H diffusion in the UO_2 lattice.

Acknowledgements

This work was supported as a part of the Center for Materials Science of Nuclear Fuel, an Energy Frontier Research Center funded by the U.S. Department of Energy, Office of Science, Office of Basic Energy Sciences under award number FWP 1356.

References

[1] C. Ronchi, M. Sheidlin, D. Staicu, M. Kinoshita, Effect of burn-up on the thermal conductivity of uranium dioxide up to 100.000 MWdt-1, J. Nucl. Mater. 327 (2004) 58.
[2] P. Gracia, G. Martin, C. Sabathier, G. Carlot, A. Michel, P. Martin, B. Dorado, M. Freyss, M. Bertolus, R. Skorek, J. Noirot, L. Noirot, O. Kaitasov, S. Maillard, Nucleation and growth of intergranular defect and insoluble atom clusters in nuclear oxide fuels, Nucl. Instrum. Methods Phys. Res. B 277 (2012) 98.
[3] G. Sattonnay, L. Vincent, F. Garrido, L. Thome, Xenon versus helium behavior in UO_2 single crystals: a TEM investigation, J. Nucl. Mater. 355 (2006) 131.
[4] L.F. He, M. Gupta, C.A. Yablisky, J. Gan, M.A. Kirk, X.-M. Bai, J. Pakarinen, T.R. Allen, In situ TEM observation of dislocation evolution in Kr-irradiated UO_2 single crystals, J. Nucl. Mater. 443 (2013) 71.
[5] S. Zinkle, Effect of H and He irradiation on cavity formation and blistering in ceramics, Nucl. Instrum. Methods Phys. Res. B 286 (2012) 4.
[6] D. Sherman, D. Olander, Hydrogen dissolution in and release from nonmetals - I. Uranium dioxide, J. Nucl. Mater. 166 (1989) 307.
[7] W. Weber, Ingrowth of lattice defects in alpha irradiated UO_2 single crystals, J. Nucl. Mater. 98 (1981) 206.
[8] G. Guimbretiere, L. Desgranges, A. Canizares, G. Carlot, R. Caraballo, C. Jegou, F. Duval, N. Raimboux, M. Ammar, P. Simon, Determination of in-depth damage profile by Raman line scan in a pre-cut He^{2+} irradiated UO_2, Appl. Phys. Lett. 100 (2012) 251914.
[9] S. Conradson, D. Manara, F. Wastin, D. Clark, G.M.L. Lander, J. Rebizant, V. Rondinella, Local structure and charge distribution in the UO_2–U_4O_9 system, Inorg. Chem. 43 (2004) 6922.
[10] J. Pang, W. Buyers, A. Chernatynskiy, M. Lumsden, B.P.S. Larson, Phonon lifetime investigations of anharmonicity and thermal conductivity of UO_2 by neutron scattering and theory, Phys. Rev. Lett. 110 (2013) 157401.
[11] "www.srim.org", [Online].
[12] R. Stoller, M. Tolozko, G. Was, A. Certain, S. Dwaraknath, F.A. Garner, On the use of SRIM for computing radiation damage exposure, Nucl. Instrum. Methods Phys. Res. B 310 (2013) 75.
[13] R. Guinebretiere, X-ray diffraction by polycrystalline materials, ISTE Ltd, Newport Beach, CA, USA, 2007.
[14] V. Rondinella, T. Wiss, The high burn-up structure in nuclear fuel – review article, Mater. Today 13 (2010) 24.
[15] V. Wheeler, The diffusion and solubility of hydrogen in uranium dioxide single crystals, J. Nucl. Mater. 40 (1971) 189.
[16] K. Lay, Oxygen chemical diffusion coefficient of uranium dioxide, J. Am. Ceram. Soc. 53 (1970) 369.
[17] R. McEachern, P. Taylor, A review of the oxidation of uranium dioxide at the temperatures below 400 °C, J. Nucl. Mater. 254 (1998) 87.
[18] J. Spino, P. Peerani, Oxygen stoichiometry shift of irradiated LWR-fuels at high-burn-ups: review of data and alternative interpretation of recently published results, J. Nucl. Mater. 375 (2008) 8.